

Preliminary performance of Sub-Surface Radar for the EJSM/Laplace mission

G. Alberti, S. Mattei
C.O.R.I.S.T.A.
Via J. F. Kennedy 5, I-80125, Naples, Italy
e-mail alberti@unina.it

L. Bruzzone, A. Ferro
University of Trento
Via Sommarive 14, I-38123, Trento, Italy

Angelo Olivieri
ASI - Space Geodesy Centre "Giuseppe Colombo"
Località Terlecchia, 75100 Matera (MT), Italy

Roberto Seu
University "La Sapienza"
Via Eudossiana 18, I-00184, Rome, Italy

R. Orosei
INAF/IFSI
Via Fosso del Cavaliere 100, I-00133, Rome, Italy

C. Catallo
Thales Alenia Space Italia
Via Saccomuro, 24, I-00131, Rome, Italy

Abstract—The Sub-Surface Radar (SSR) instrument is a core payload for the Jupiter Ganymede Orbiter (JGO) of the EJSM, which is complementary to the Ice Penetrating Radar on board the Jupiter Europa Orbiter (JEO). These instruments work at low frequency (HF/VHF band) and are designed to penetrate the surfaces of icy moons of Jupiter. The paper will present a preliminary performance model aimed to assess the penetration capability of the instrument in different operative conditions and planet's surface characteristics.

Keywords—Sub-sounder, planetary exploration, performance model, SNR, clutter

I. INTRODUCTION

The Europa Jupiter System Mission (EJSM) is one of the major joint European Space Agency (ESA) and NASA missions in the Solar System currently under study. It is aimed at exploring Jupiter and its icy moons with two spacecrafts having different complementary goals: the Jupiter Europa Orbiter (JEO), provided by NASA and devoted to study Jupiter and the Jovian moons Io and Europa, and the Jupiter Ganymede Orbiter (JGO), which represents the contribution of ESA and will investigate Jupiter and the Ganymede and Callisto moons.

The core payloads of both platforms include a radar sounder instrument. Radar sounders are active instruments (similar in concept to terrestrial ground penetrating radars) that are based on the transmission of radar pulses at frequencies in the MF, HF and VHF portions of the radio spectrum into the surface and the subsurface. The detected echoes are processed in order to construct radargrams that contain detailed information on the subsurface structure, pointing out the main interfaces between different layers. Radar sounders are particularly effective on ice and, therefore, suitable for investigating the subsurface of the Jupiter icy moons.

These instruments can exploit the common heritage from the radar sounders developed for two recent Mars missions: Mars Advanced Radar for Subsurface and Ionosphere

Sounding (MARSIS) on ESA's MARS Express [1], and Mars Shallow Radar Sounder (SHARAD) on NASA's Mars Reconnaissance Orbiter [2]

This paper focuses on the SSR performance taking into account possible orbital parameters and planet's surface features. The signal power received by superficial and sub-superficial layers is evaluated and compared with main noise sources: thermal, surface clutter and cosmic and Jovian's radio emission. In this way it is possible to derive the main system performance, mainly in terms of its penetration capability and, therefore, to determine optimal radar parameters through necessary trade-offs.

II. INSTRUMENTS ARCHITECTURE

Instrument concept is enforced by experiences gained in the two successful precursor missions on Mars, i.e. MARS Express, with the MARSIS instrument, and NASA Reconnaissance Orbiter with SHARAD. It has been proved that radar sounder systems at low frequency (HF/VHF band) are able to penetrate the planet's surface and to perform a sub-surface analysis with a high vertical resolution (in the order of some meters).

Also the design of the instrument can follow that used for SHARAD [3] that has allowed a very straightforward operation of the radar. A generic block diagram of the foreseen architecture is provided in Figure 1.

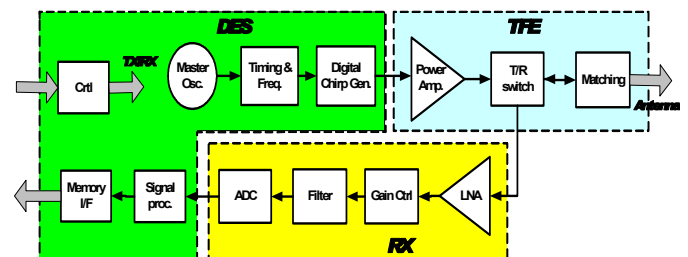


Figure 1. Architecture of the Sub-Surface Radar Instrument

The Digital Electronics Sub-system (DES) envelopes the Command and Control functions interfacing with the spacecraft bus, the processing capabilities to pre-elaborate the science data collected during the observations, as well as the digital synthesis of the radar pulse and generation of the system timings. The frequency modulated radar pulses are digitally generated directly at the transmit frequency so that no conversion is needed. Signal is amplified at the required power level before being sent to the antenna matching network within the Transmit Front-End (TFE). The receiving sub-system (RX) uses a direct conversion approach with downsampling.

III. PRELIMINARY PERFORMANCE MODEL

For a nadir-looking sub-sounder the main performance figure is related to its penetration capability that depends on the power ratio between the signal coming from a generic sub-surface interface (a change in the dielectric constant) and, generally speaking, noise coming from every disturbing and unwanted signal sources. Signal power (S) can be evaluated by using a classic “radar equation” that expresses the received power by a generic radar as a function of transmitted power (P_T), antenna gain (G), wavelength (λ), radar altitude (H) and surface radar cross section (σ_s), i.e.:

$$S = A\sigma_s \quad (1)$$

$$A = \frac{P_T \lambda^2 G^2}{(4\pi)^3 H^4} \quad (2)$$

Target radar cross section can be expressed by the product of surface backscattering coefficient (σ^0) and illuminated area that, in this case, can be approximated by the pulse-limited circle, i.e.:

$$\sigma_s = \pi \frac{Hc}{B} \sigma^0(\theta) \quad (3)$$

where c is the speed of light and B is the transmitted bandwidth.

Planet’s terrain is supposed to be a random rough process and a fractal geometry is considered since it has been proved [4] to be the most suitable method for describing natural surfaces. In this way, a closed form for the backscattering coefficient can be derived under the Kirchhoff approach and the small-slope approximation [5]:

$$\sigma^0(\theta) = 2k^2 \rho'(\theta) \cos^2 \theta \int_0^\infty J_0(2k\tau|\sin \theta|) \exp(-2s^2 k^2 \tau^2 \cos^2 \theta) dt \quad (4)$$

where $k = 2\pi/\lambda$ is the wavenumber, θ is the incidence angle, H is the Hurst coefficient and s is a parameter related to the characteristic length of the surface called topohesy.

$$s = T^{(1-H)} \quad (5)$$

end $\rho'(\theta)$ is the Fresnel power reflection coefficient for the horizontally polarized wave:

$$\rho'(\theta) = \left| \frac{\cos \theta - \sqrt{\epsilon'_r - \sin^2 \theta}}{\cos \theta + \sqrt{\epsilon'_r - \sin^2 \theta}} \right|^2 \quad (6)$$

where ϵ'_r is the surface relative permittivity.

The last expression for the backscattering coefficient exhibit interesting similarities to other models when $H=0.5$ or $H=1$ [6].

When signal power coming from a sub-surface, at depth Δ , shall be evaluated also the attenuation of the crossed terrain layer should be considered such as:

$$\Gamma = [1 - \rho'(0)]^2 \sigma_{ss}(0) \exp(-\alpha_{TOT}) \quad (7)$$

where σ_{ss} is the sub-surface radar cross section that has similar expression of (3) but considering different Fresnel power reflection corresponding to the sub-surface layer with relative permittivity ϵ''_r

$$\rho''(\theta) = \left| \frac{\sqrt{\epsilon'_r} \cos \theta - \sqrt{\epsilon''_r - \epsilon'_r \sin^2 \theta}}{\sqrt{\epsilon'_r} \cos \theta + \sqrt{\epsilon''_r - \epsilon'_r \sin^2 \theta}} \right|^2 \quad (8)$$

and α_{TOT} is the total two-way attenuation of terrain layer, given by:

$$\alpha_{TOT} = 2 \int_0^\Delta \alpha(1) dl \quad (9)$$

Models for estimating the foreseen attenuation as a function of ice depth on Jupiter’s icy satellites can be found in the literature [9], [10]. An example of possible ice attenuation as a function of penetration depth for two carrier frequencies (20 MHz and 50 MHz) is shown in

Figure 2, by supposing an ice superficial temperature of 100 K.

For signals also compression factor in either range and azimuth should be considered, for taking into account coherent integration:

$$\eta = \frac{PRF}{B_D} \frac{H\lambda B\tau}{2\rho_{az}^2} \quad (10)$$

where ρ_{az} is the achievable azimuth resolution, τ is the transmitted pulse length, B is the transmitted bandwidth and PRF is the pulse repetition frequency.

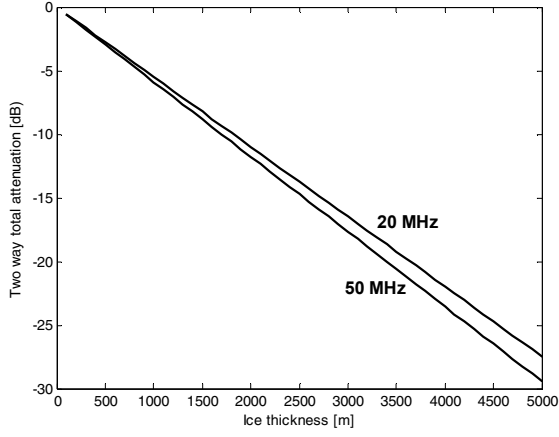


Figure 2. Ice attenuation based on Chyba model (ice superficial temperature of 100 K)

The noise contributions arise from thermal noise, surface clutter, and environmental noise and each term contributes to a different Signal-to-Noise ratio.

The first ratio is related to thermal noise:

$$N = KT_sBF \quad (11)$$

where K is the Boltzmann constant, T_s the system temperature and F the receiver noise figure and it is given by:

$$SNR_{th} = \frac{A\Gamma\eta}{N} \quad (12)$$

The second ratio refers to the fact that the surface echo coming from lateral directions (off-nadir clutter) may interfere with the subsurface echo in the same range cell. The basic equations for evaluating this so called signal to clutter ratio (SCR) can be found in the literature [4], [8] and it reaches the following expression:

$$SCR = \frac{A\Gamma}{S(\bar{\theta})} \quad (13)$$

where:

$$\bar{\theta} \approx \sqrt{\frac{2\Delta\sqrt{\epsilon'_r}}{H}} \quad (14)$$

The last term of noise is the most relevant and it is related to background radio noise that is strongly different from that experienced on Mars as the classic galactic noise is sharply below the Jupiter's radio emission (see Figure 3). By considering an equivalent noise temperature for either cosmic (T_c) and Jupiter (T_j) radio noise, the noise contribution in the Jovian (N_j) and Anti-Jovian part (N_{AJ}) of the orbit can be evaluated as:

$$\begin{aligned} N_j &= KT_jBF\bar{\rho} \\ N_{AJ} &= KT_cBF \end{aligned} \quad (15)$$

where $\bar{\rho}$ is the surface albedo. The corresponding signal to noise ratios are therefore:

$$\begin{aligned} SNR_j &= \frac{A\Gamma\eta}{N_j} \\ SNR_{AJ} &= \frac{A\Gamma\eta}{N_{AJ}} \end{aligned} \quad (16)$$

This effect can only be mitigated by the antenna pattern and depends on orbit characteristic (Jovian and anti-Jovian positions) and satellite attitude.

On the basis of the previous expressions, a suitable instrument performance model can be developed. The architecture and the foreseen input and output variables are shown in Figure 4.

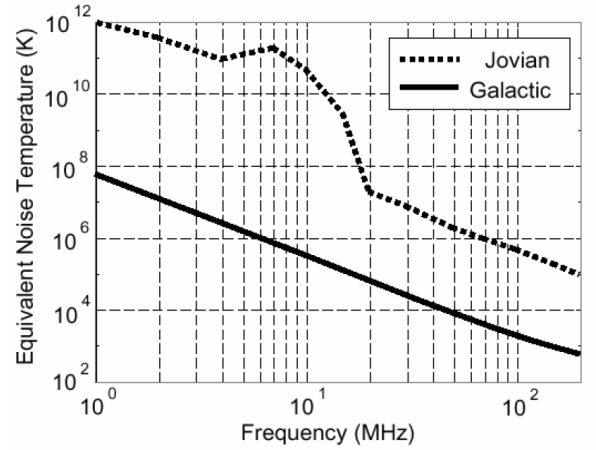


Figure 3. Jovian and galactic noise temperatures as a function of frequency

IV. PERFORMANCE EVALUATION

A preliminary radar definition and evaluation of performance is reported in the following as an example in order to better underline various effects of radar parameters on overall performance and possible trade-off.

Being the Jovian background noise the most critical source of disturbing signal and taking into account its behavior as a function of frequency (see Figure 3), the choice of operating frequency is oriented on high values also taking into account that ice attenuation is almost constant up to hundreds of MHz.

For example, for a carrier frequency of 50 MHz, by using the previous attenuation values and assuming suitable input parameters needed for the performance model of Figure 4, it is possible to evaluate signal power coming for various subsurface layers as well as noise power due to Jovian emission, thermal effects and surface clutter as shown in Figure 5.

In particular the first group of curves on the lower part of the plot represents layers with low dielectric contrast (few

tenths of variation) while the second group on the upper part of the plot those with high dielectric contrast (from 5 up to 87 of dielectric constant). The first group of layers can represent stratigraphy due to small changes of ice constitution while the second group refers to solid interfaces of various material including liquid water (87 of dielectric constant).

up to about 3000 m in the Jovian part and 4000 m in the anti-Jovian part of the orbit.

An important role is played by PRF and pulse duration values that both can significantly increase the overall radar SNR and, therefore, improve its detection capability. In this case a PRF of 500 Hz and a pulse duration of 150 μ sec have been considered.

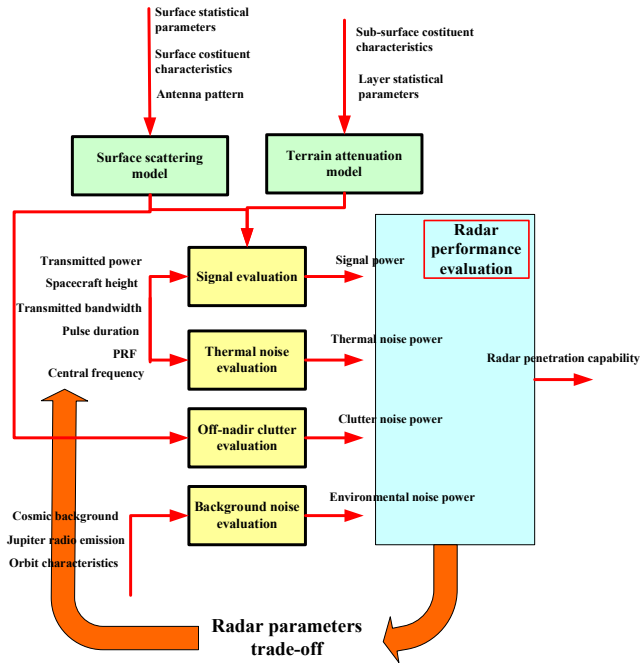


Figure 4. Instrument performance model

In this example case the antenna is supposed to be a single dipole (about 5 m long) and the surface is very smooth implying a low level of off-nadir clutter power.

By a rapid view of Figure 5 it is possible to infer that the radar is able to detect stratigraphy with low dielectric contrast only in the anti-Jovian part of the orbit up to about 500 m while layers with high values of dielectric constant can be detected

REFERENCES

- [1] G. Picardi, and 12 colleagues. «MARSIS: Mars Advanced Radar for Subsurface and Ionosphere Sounding.» En Mars Express: the scientific payload, de A. Wilson, 51-69. Noordwijk, Netherlands: ESA Publications Division, 2004.
- [2] Seu, R., Phillips, R. J., Biccari, D., Orosei, R., Masdea, A., Picardi, G., Safaenili, A., Campbell, B. A., Plaut, J. J., Marinangeli, L., Smrekar, S. E., and Nunes, D. C. «SHARAD sounding radar on the Mars Reconnaissance Orbiter.» J. Geophys. Res., n° 112 (2007b): E05S05.
- [3] R. Croci, F. Fois, D. Calabrese, E.M Zampolini, R. Seu, G. Picardi, E. Flamini, «SHARAD Design and Operation», Geoscience and Remote Sensing Symposium, 2007. IGARSS 2007.
- [4] B. B. Mandelbrot, «The Fractal Geometry of Nature», New York: Freeman, 1983.
- [5] G. Franceschetti, A. Iodice, M. Migliaccio and D. Riccio, «Scattering from Natural Rough Surfaces Modeled by Fractional Brownian Motion Two-Dimensional Processes», IEEE Transactions on Antennas and Propagation, vol. 47, no. 9, September 1999
- [6] M. K. Shepard, B. A. Campbell, «Radar Scattering from a Self-Affine Fractal Surface: Near-Nadir Regime», Icarus 141, 156–171 (1999)
- [7] G. Picardi, D. Biccari, R. Seu, L. Marinangeli, W.T.K. Johnson, R. L. Jordan, J. Plaut, A. Safaenili, D. A. Gurnett, G. G. Ori, R. Orosei, D. Calabrese and E. Zampolini, «Performance and surface scattering models for the Mars Advanced Radar for Subsurface and Ionosphere Sounding (MARSIS)», Planetary and Space Science, n° 52 (2004): 149–156.
- [8] R. Seu, D. Biccari, R. Orosei, L. V. Lorenzoni, R. J. Phillips, L. Marinangeli, G. Picardi, A. Masdea and E. Zampolini, «SHARAD: The MRO 2005 shallow radar», Planetary and Space Science, n° 52 (2004): 157–166.
- [9] C. F. Chyba, S. J. Ostro and B. C. Edwards, «Radar Detectability of a Subsurface Ocean on Europa» Icarus, n° 134 (1998): 292-302.
- [10] J. C Moore, «Models of Radar Absorption in European Ice», Icarus, n° 147 (2000): 292-300.

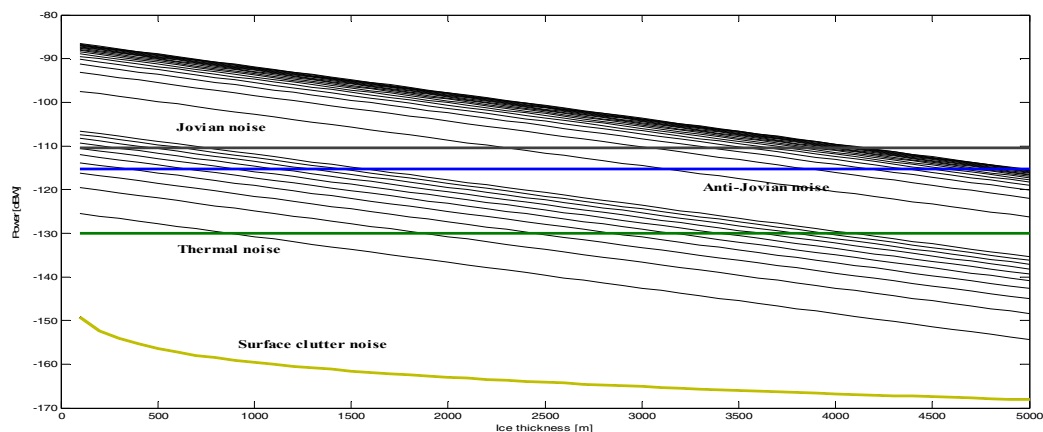


Figure 5. Subsurface signal and noise power